Underwater Acoustics and Fourier Analysis

E80: Section 4, Team 5 – February 9, 2018
Vicki Moran

Abstract*— This paper details the process of designing and constructing circuit interfaces to a microphone and a speaker in order to perform underwater position measurements. Standard amplifying circuits were used to amplify the signals received and sent by the instruments in order to generate clearer signals for analysis. The speaker and microphone were then placed in the test tank to measure distance using two different methods. One method involved triangulating based on calibration curves of power received from three beacons emitting various frequencies. The other more reliable method called for time of flight measurements, which took advantage of burst modulation and the speed of sound in water. Fourier analysis better explained the behavior of these signals, so an oscilloscope and Matlab were used to find the FFT of various signals. Experimental results demonstrate that the time of flight measurements produced more reliable data, producing the relationship *distance = 1400*time – 0.047.

I. Introduction

Underwater acoustics refers to the propagation of sound in water and the interaction of these acoustic waves with subaqueous environments. While sound travels at a speed of about 343m/s in air, this speed is scaled by a factor of over four to about 1,484m/s in water; however, this value differs based on temperature, salinity and pressure [4]. Due to these unique transmission characteristics, humans struggle to perceive sound underwater. Various instruments overcome this barrier by taking advantage of the qualities of sound propagation in water to send and receive audio signals. These instruments are used to take measurements that can be useful in describing an underwater environment.

Distance can be measured using underwater acoustics through amplitude decay and time of flight techniques. Sound is a wave, and therefore propagates, spreads, and reflects. These waves carry power, which is inversely related to the radius squared through the relationship $P_{received} \propto I(r) = \frac{P_{transmitted}}{4\pi r^2}$. Though waves can be attenuated, calibrating the relative power from a speaker at different distances can give valuable information about location. Waves also reflect off surfaces, so the distance traveled to a surface can easily be calculated from knowledge of the speed of the wave and calculations of the time of flight.

This lab involves designing circuit interfaces to a speaker and microphone that can be used underwater to take position measurements using the methods described above. Since the voltage received by the microphone is best interpreted in the frequency domain, Fourier analysis will be useful for understanding the signal behavior [1]. A Fourier transform essentially uses several sinusoids of various frequencies and amplitudes to represent a signal. The Fast Fourier Transform (FFT) used in this lab is an algorithm that deconstructs signals into discrete components in the frequency domain. The peaks of FFT plots show which frequencies of sinusoids are present.

II. Elements

A. *Dayton DAEX25W-8 Audio Exciters* – This waterproof speaker has an impedance of 8Ω and RMS power handling of 10W [7].
B. *LM384 Audio Amplifier* – The LM384 power audio amplifier has an internally fixed gain of 34dB, which correlates to a voltage gain of 50. With a supply range of 12V to 26V and an input impedance of 150kΩ, this amplifier can significantly increase the power driven through a speaker [8].
C. *CME-1538-100LB Electret Microphone* – This waterproof microphone operates with a maximum voltage of 10V and has an output impedance of 2.2kΩ.

III. Fast Fourier Transform

All signals can be represented as the sum of a series of sinusoids. To better understand the effects that changing the drive signal and windowing has on a FFT, the math function of the Agilent/Keysight 2024A oscilloscope was used to display the FFT of various signals.

A. Sinusoidal Wave

The first wave that was driven into the oscilloscope was a 11kHz sine wave with an amplitude of 1.5V. Because a sine wave is already a sinusoid, the expected FFT is a single peak occurring at the frequency of the wave. This outcome can be seen in the plot shown in Figure 1.

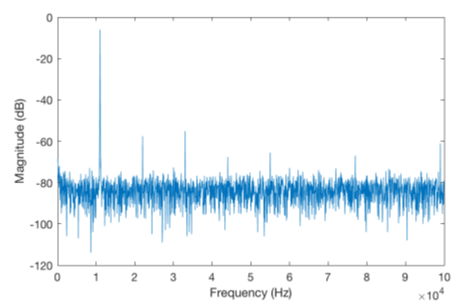

Figure 1: FFT of a 11kHz sine wave drive signal.

Although there is a significant amount of noise, there is a clear peak occurring at 11kHz. Changing the frequency of the sine wave will shift the peak of the FFT to occur at that new frequency value.

B. Square Wave

An ideal square wave can be represented as an infinite sum of sinusoidal waves. Using Fourier expansion, an ideal square wave can be represented as

$$y = \frac{4}{\pi}\sum_{k=1}^{\infty}\frac{\sin(2\pi(2k-1)ft)}{2k-1} \quad [9].$$

This summation only includes sine waves with frequencies that are odd multiples of the cycle frequency *f*. Therefore, the ideal square wave should only have odd harmonic frequencies. This can be visualized with the series of sine waves shown in Figure 2.

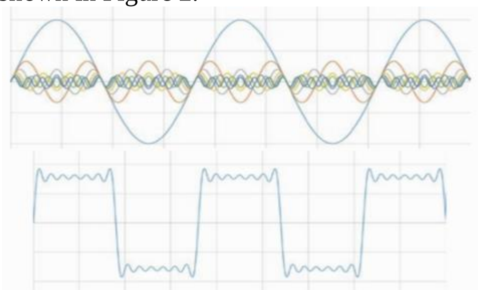

Figure 2: Square wave as sum of harmonic sine waves [10].

The following plot in Figure 3 shows the FFT of an 11kHz square wave displayed by an oscilloscope.

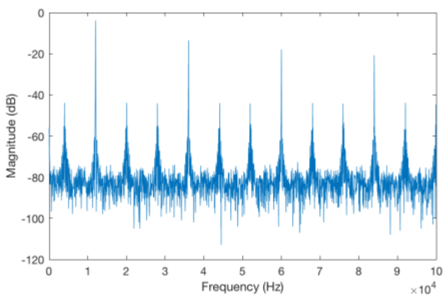

Figure 3: FFT of a square wave drive signal.

The prominent peaks in Figure 3 occur at frequencies within ten kilohertz of the expected values 11kHz, 33kHz, 55kHz, and 77kHz. However, several other arbitrary peaks appear which may have resulted from approximations of the square wave produced by the function generator. Another source of this error may have been that the FFT function of the oscilloscope could not distinguish between the harmonics and other erroneous frequencies, some of which may have resulted from rectangular windowing, as described in the next section.

C. *Windowing*

The FFT transform assumes that a finite data set spans an integer number of periods of a periodic signal. When the number of periods recorded is not an integer, the result is a truncated waveform with artificial discontinuities. This discontinuity results in non-periodicity that the oscilloscope interprets as a high frequency which is not actually a part of the signal. This jump occurs when using a standard rectangular window as evident in Figure 4.

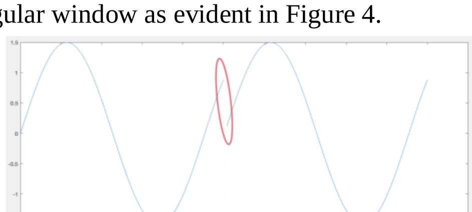

Figure 4: Non-periodicity of signal with rectangular window.

Windowing can eliminate these discontinuities by scaling all values by a window whose amplitude decreases gradually and smoothly to zero at the edges. The Hanning window can be applied to these signals, as shown in Figure 5 to greatly reduce spectral leakage and increase frequency resolution [10].

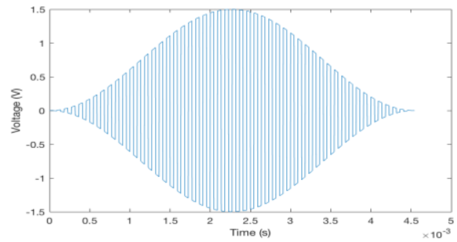

Figure 5: Square wave in time domain with Hanning window.

This Hanning window was applied in Matlab using the command hann(L) with the line of code

```
data = data'.*hann(2000);.
```

Changing the window on the 11kHz square wave from rectangular to Hanning on the oscilloscope produces the FFT in Figure 6.

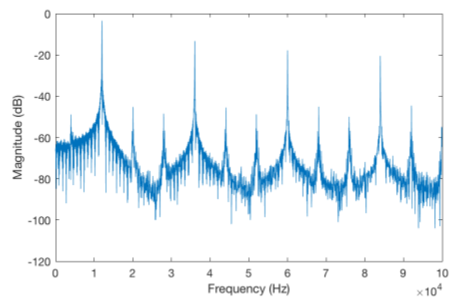

Figure 6: FFT of a square wave drive signal with a Hanning window.

With the Hanning window, the prominent peaks are much clearer than in Figure 3, and the noise is reduced.

D. *Matlab Analysis*

The Matlab code, as given in Appendix 1, was applied to take the FFT of the time-domain oscilloscope data. This code can be modified to plot either the FFT index or the angular frequency in radians per second on the x-axis rather than the frequency in hertz.

The CSV data from the oscilloscope, however, only saved the FFT of the signals, so this Matlab code was instead applied to a simulated ideal square wave.

By modifying line 2 of the code in Appendix 1 to be

```
2:  t = 0:0.000002273:0.0045454545;
```

and line 6 to use the square function of Matlab,

```
6:  data = 1.5*square(69115*t);
```

the FFT function can be applied to generate the plot of the FFT as shown in Figure 7.

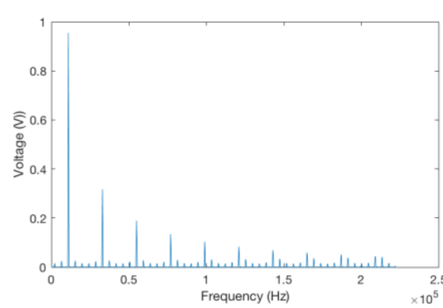

Figure 7: Matlab FFT of ideal square wave.

The FFT of the square wave generated by the oscilloscope follows the trends shown in this Matlab plot but contains more extraneous peaks and noise.

E. *Discrete and Sampled Continuous*

Since measurement devices and computational programs can only record distinct data points, the FFT can only be plot as a discrete or sampled continuous signal. While both of these are considered Discrete Fourier Transforms, a discrete signal is plot against sample number while a sampled continuous signal is plot against time. For an 11 kHz square wave, the former can be seen in Figure 8, using the Matlab code given in Appendix 2, while the latter in Figure 7.

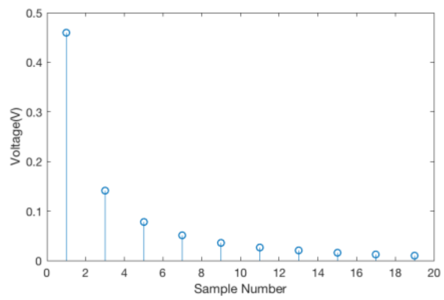

Figure 8: Discrete FFT of ideal square wave.

The discrete plot shows the magnitudes at odd multiples of the sample number, while the continuous plot shows magnitudes at frequently sampled times.

F. *Sampling Rate and Time Scale*

The sampling rate of the FFT changes based on the time scale set on the 2024A oscilloscope. The scope has a maximum memory of 1000 kilosamples, so the sample number is fixed at that value. It is evident that

$$sample\ number = sample\ rate * time\ scale,$$

which shows that the sample rate and time scale are inversely related. Therefore, decreasing the time scale increases the sample rate and thus the FFT resolution.

IV. DESIGN

A. *Circuit Interfaces to Speakers*

The Dayton Audio Exciter converts a voltage input to an audio output. This speaker has an input impedance of only 8Ω and the 33120A signal generator has a resistance of 50Ω, so in the equivalent circuit model, the combined resistance of these in series is 58Ω. The signal generator can output a maximum peak voltage of 10V, so the current through the speaker can be found as $I = \frac{V}{R} = \frac{10\text{V}}{58\Omega} = 0.17\text{A}$. It follows that the sustained power that can be driven through the speaker is $P = I^2R = (0.17\text{A})^2(8\Omega) = 0.119\text{W}$. This demonstrates the need for an amplifying circuit interface using the LM384 audio amplifier, which can drive an instantaneous peak power of 7.78W. The design for the circuit interface to the speaker is given in the LM384 audio amplifier data sheet, shown in Figure 9.

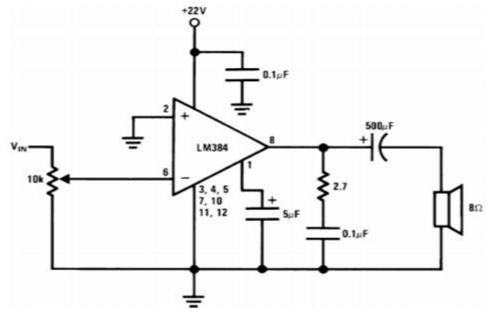

Figure 9: Typical 5W amplifier reference design [8].

The 10kΩ potentiometer in this reference design can control the volume emitted by the speaker. Decreasing the resistance of the potentiometer increases the volume, so the resistance and volume are inversely related. However, since the use of the speaker in this lab is limited to generating the voltage signal with the function generator, the volume can simply be controlled by adjusting the peak to peak voltage of the input signal.

AC Coupling is a technique that involves driving an output through a series capacitor [1]. The circuit in Figure 9 employs this technique by placing a 500μF capacitor in series with the speaker. This prevents damage from DC current by stopping DC and lets high frequencies through to create the desired audio response. An additional 4.7μF bypass capacitor is placed on the supply rails in order to add stability and remove noise.

To better understand the need for the amplification from the LM384, a 20 kHz, 190mVpp signal was driven into both the speaker alone and the speaker with the AC coupled LM384. With only the speaker, the power dissipated was measured to be 12mW, while with the circuit interface, the power dissipated was 32W. This shows that the audio amplifier is necessary for outputting higher levels of power through the speaker.

B. *Circuit Interfaces to Microphones*

The CME-1538-100LB microphone picks up a sound input and amplifies this signal with a gain of 100 to generate a voltage output. The reference circuit to amplify the input to the microphone is shown in Figure 10 below.

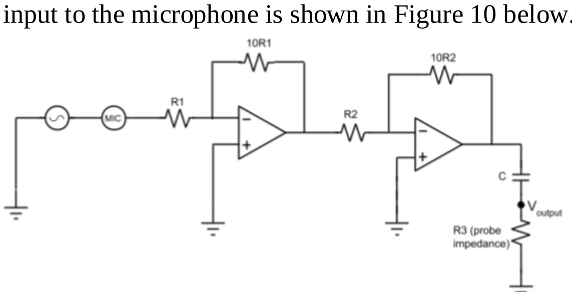

Figure 10: Reference circuit for electret microphone.

The coupling capacitor along with the probe impedance act as a high pass filter to remove any low frequency noise from the data. Since the cutoff frequency is inversely related to the 9MΩ impedance of the probe and the capacitance, if we set the cutoff frequency to 1000Hz, then $C = \frac{1}{9\text{M}\Omega * 1\text{kHz}}$ =11nF.

The circuit AC couples the output by placing a capacitor in series. Because AC coupling is used, DC offset is removed, so the output signal is centered around 0V. Therefore, a dual-rail op-amp is necessary for preserving the positive and negative parts of the signal.

To achieve a gain of 100, two stages each with a gain of 10 must be cascaded due to the limitations set by the gain-bandwidth product of the op-amp. Bandwidth refers to the range of frequencies that generate a voltage gain of above 70.7% of the maximum output value, calculated as

$$bandwidth = \frac{GBP}{gain}.$$

For the OP07 operational amplifier used in this circuit, the GBP is given as 0.6MHz [13], so the bandwidth with a gain of 100 is $\frac{0.6\text{MHz}}{100} = 6000\text{Hz}$. This means that only frequencies within the range of 1kHz, the cutoff frequency set by the capacitor, to 6kHz will have a gain of above 70.7. However, the speaker should allow frequencies up to at least 20kHz to pass, which this bandwidth would not allow. Therefore, reducing the gain to 10 would change the bandwidth to $\frac{0.6\text{MHz}}{10} = 60\text{kHz}$, which is a much more appropriate bandwidth given the expected frequencies.

V. EXPERIMENTS

Several methods can be employed to locate a robot using underwater acoustics. A series of experiments were performed in the test tank to acquire distance measurements using two of these methods.

The first measurement involved triangulating the position of the microphone based on the power received from three beacons. Each beacon constantly emitted sine waves with different frequencies. The east, southwest, and northwest beacon gave off signals of 10kHz, 11kHz, and 12kHz, respectively. Measuring the voltage received by the microphone at varying locations throughout the tank showed the relative power from each beacon. The FFT was used to separate out the contributions from each beacon and to create a calibration curve relating the received power and distance from each beacon.

The second measurement used time of flight range finding to determine the distance from a wall of the tank. Burst modulation, a feature of the old signal generators, was used to send short pulses out from the speaker, and the microphone picked up these pulses. The HP/Agilent 33120A function generator sent a triggered burst of five 19kHz sine waves at a frequency of 5Hz, so five bursts were sent each second. Measuring the distance between peaks of the acoustic output sent from the speaker and the corresponding voltage received by the microphone showed the time of flight. Performing this measurement at different measured distances from the wall produced a calibration curve relating distance and time of flight.

VI. RESULTS

A. *Distance Measurement: Amplitude Decay*

The microphone was placed at five locations throughout the tank, and power amplitude measurements were taken at each of these positions. To calculate the power from each beacon, the FFT was computed to separate out the voltage contributions from each speaker. For one of the positions, the FFT plot is shown in Figure 11, with relevant peaks around 10kHz, 11.4kHz, and 12kHz corresponding to the frequencies emitted by each beacon.

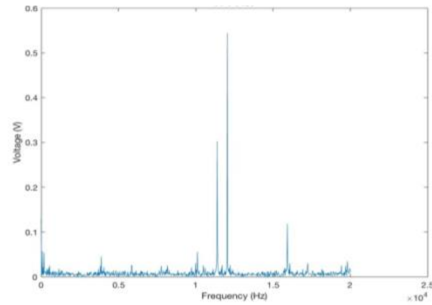

Figure 11: FFT plot of voltage amplitude from three beacons.

The oscilloscope records the magnitude at each frequency in decibel-volts, so the magnitudes were first converted to voltages using the equation $V = 10^{\frac{X_{dBV}}{10}}$ [2]. Then, voltage and pressure are linearly related, so $P \propto V^2$; therefore, squaring the voltage gives a measurement that is proportional to power. This value is plotted again distance in Figure 12 for each data point recorded. All values can be plotted on the same graph because the frequency should not affect the power received.

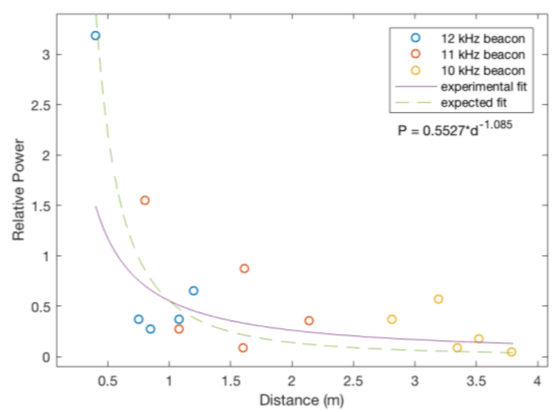

Figure 12: Relative power versus distance calibration curve.

The expected relationship between power and distance is $P \propto \frac{1}{d^2}$. The experimental data was fit with a curve $P = 0.5527 * d^{-1.085}$ using Matlab's fitting tools. The expected fit is also shown in Figure 12 by the dashed green line, which seems to loosely correlate with the data.

Large deviations in this calibration curve resulted from several sources of error. Quantifying the error is beyond the scope of this lab, but it derives from echoing in the tank, attenuation of waves into heat, and inaccuracy of measurement devices.

B. *Distance Measurement: Time of Flight*

Time of flight is another acoustic measurement technique to determine position that relates the time for a signal to travel to a wall and back and the distance traveled based on the speed of sound. Approximating this speed in water as 1,484m/s, the expected time of flight for each round trip distance can simply be calculated as

$$time_{expected} = distance \,/\, (1484 \tfrac{\mathrm{m}}{\mathrm{s}}).$$

For each measured distance away from the wall, the calculated expected time is shown in Table 1.

To measure the time of flight, the microphone was placed on a PVC pipe next to a speaker and immersed underwater. The trigger output of the function generator synchronized the sample timing of the oscilloscope and function generator. Then, the oscilloscope was set to normal mode acquisition and the averaging function was applied to the received signal to cancel noise and other signals. The time of flight was measured on the oscilloscope by using the cursors to find the time difference between the start of the speaker output burst and the start of the corresponding signal received by the microphone, as shown in Figure 13.

Figure 13: Triggered oscilloscope snapshot of burst sent and received.

The extraneous waves in the received signal likely resulted from multipath, causing multiple echoes and interference.

The following table shows the measured time for six different round trip distances compared to the calculated expected times.

Distance to Detection (m)	Expected Time (ms)	Measured Time (ms)
0.2032	0.138	0.21
0.6604	0.448	0.34
0.9144	0.62	0.578
1.2192	0.827	0.866
1.5748	1.07	0.112
1.7272	1.17	0.118

Table 1: Round trip distance and time of flight data.

These values were plotted to create a calibration curve of distance versus time of flight shown in Figure 14. Error primarily came from inaccuracies in measurements of the distance traveled, accurate within a range of $\pm$ 0.05 m.

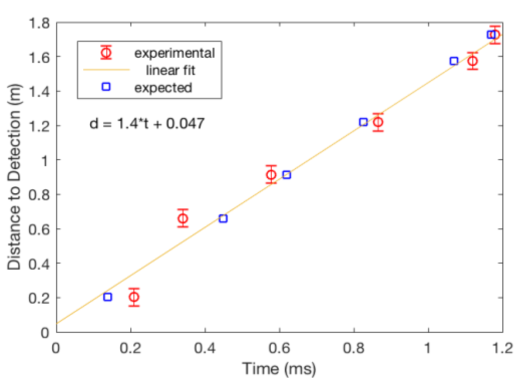

Figure 14: Distance versus time of flight calibration curve.

With a linear fit, the relationship between time of flight and distance using the experimental data is found as $distance = 1.4 * time + 0.047$.

VII. Conclusion

Underwater acoustics is a valuable tool for taking position measurements, as seen through the results of this lab. Using amplitude measurements for range finding produced a power and distance calibration curve with an inverse squared relationship. However, this method produced large uncertainties and variations in power, bringing into question its reliability. Furthermore, since the power amplitude decreases so quickly, the range of distances is very limited. Time of flight is a much more reliable method for acoustic measurements as long as there is a surface large enough to reflect the transmitted signal.

These acoustic methods for determining position have many broader applications, from mapping the wreckage of a plane crash to tracking fish with acoustic tag. More relevant to the scope of E80 is the use of acoustics for tracking a beacon or mapping depth in the final project. Overall, underwater acoustics is useful for a wide variety of measurements and Fourier analysis allows for a better understanding of the results.

References

[1] "Lab 3: Operational Amplifiers and Marine Sensors," *E80 - Experimental Engineering*, Harvey Mudd College. [Online].

[2] "Underwater Acoustics," *E80 - Experimental Engineering*, Harvey Mudd College. [Online].

[3] M. S. Ballard, "Underwater Acoustics," *Acoustics Today*, 02-Dec-2017. [Online].

[4] "The Underwater Propagation of Sound and its Applications," *DUJS Online*, 10-Nov-2013. [Online].

[5] *Keysight InfiniiVision 2000 X-Series Oscilloscopes User's Guide*, Keysight Technologies. 2013.

[6] *Agilent 33120A User's Guide*, Agilent Technologies, Inc. 2002.

[7] *DAEX25W-8 Audio Exciter Spec Sheet*, Dayton Audio. 2014.

[8] *LM384 5W Audio Power Amplifier1*, Texas Instruments. 2013.

[9] "Square Wave," *Wikipedia*. [Online].

[10] "Understanding FFTs and Windowing," *National Instruments*. [Online].

[11] *CME-1538-100LB Electret Condenser Microphone*, CUI, Inc. 2015.

[12] "Lecture 6 – Discrete Fourier," *E80 - Experimental Engineering*, Harvey Mudd College. [Online].

[13] *Ultralow Offset Voltage Operational Amplifier OP07*, Analog Devices. 2011.

APPENDIX

Appendix 1: FFT Matlab Code (shared with team)

```
% time
t = table2array(data2(:,1));
time = t(end)-t(1);
numSamples = size(t);

% voltage
data = table2array(data2(:,2));

% sampling frequency
Fs = numSamples(1)/time;

% number of samples = time * sample rate
L = time*Fs;

% fast fourier transform
Y = fft(data);

% taken from Matlab example code for FFT
% converts x-axis from FFT index to frequency
P2 = abs(Y/L);
P1 = P2(1:L/2+1);
P1(2:end-1) = 2*P1(2:end-1);
f = Fs*(0:(L/2))/L;

% plots a one-sided stem plot
plot(f,P1);
xlabel('Frequency (Hz)');
ylabel('Voltage (V)');
```

Appendix 2: Discrete Square Wave Matlab Code (written alone)

```
count = 1;
% extracts each peak at frequencies that are odd multiples of 11 kHz (or index 50)
for i=1:1001
    if mod(i-50,100) == 0
        newP1(count) = P1(k);
        count = count+1;
    end
end

% creates a stem plot at discrete integer values
k = 1:2:19;
stem(k,newP1);
xlabel('K');
ylabel('Voltage (V)');
```